

RBC elastic properties studied by means of active rheology approach

Maria D. Khokhlova, Evgeny V. Lyubin, Maria N. Skryabina and Andrey A. Fedyanin

Faculty of Physics, Lomonosov Moscow State University, Moscow 119991, Russia

ABSTRACT

Double optical tweezers combined with active rheology approach are suggested for dynamic monitoring of the red blood cell elastic properties. Frequency dependence of the phase difference in the forced movement of the erythrocyte opposite edges appeared to be highly dependent on the rigidity of the cellular membrane. Cell relaxation time value is suggested as an effective parameter determining the state of the cell. Photo-induced effects caused by optical trapping are analyzed.

Keywords: RBC elastic properties, optical trapping, active rheology

1. INTRODUCTION

Characterization of viscoelastic properties of cellular membranes is a crucial problem of tissue physiology as it gives an opportunity to detect changes caused by various diseases or drug effects. Local methods probing the cellular viscoelastic properties and characteristics of complex materials at the microscale provide tools to characterize the physiological state of the membrane and its changes and are of great practical and fundamental importance so far. The most widespread techniques to work with single cells are optical tweezers,¹⁻⁴ micropipette aspiration technique,⁵⁻⁷ and atomic force microscopy.^{8,9} These methods are based on the analysis of the cell response when it is perturbed by an external force. Recently a new method to study viscoelasticity of the red blood cell (RBC) membrane was proposed¹⁰ by attaching a functionalized ferrimagnetic microbead to the RBC membrane and exposing the system in the ac-magnetic field. The magnetic bead's motion caused the deformation of the membrane and elastic and frictional moduli were extracted from optically tracked bead motion. However the only method having the ability for ultrafine positioning, control and noninvasive probing of local object properties in aqueous solution having no impact from the bulk substrate is the optical tweezers technique which is a unique tool for exploring problems related to quantitative characterization of single objects at the microscale.¹¹⁻¹³ This technique is widely used to determine the elastic properties of cell membranes, in particular of the RBC membranes being noninvasive and handy tool for characterization of living cells. In the present work which is an extended version of Ref.¹⁴ we suggest a new way to employ optical tweezers and active rheology approach to dynamically probe viscoelastic properties of the cells. Active rheology is based on the analysis of the studied objects motion on the frequencies of external perturbations caused by optical traps. This approach is the further development of so-called passive rheology¹⁵ monitoring the thermal fluctuations of the studied object. This approach was widely used to study erythrocyte flicker effect. The term "flicker" was introduced for the phenomenon of spontaneous low-frequency oscillations of the erythrocyte membrane. This effect, in turn, is used as an important tool in the investigation of the mechanics of the cell membrane.^{16,17} Passive rheology was also used to study the effect of hydrodynamic coupling on the dynamics of two colloidal particles held in fixed optical traps.¹⁸ Here we report on a new approach to study viscoelastic properties of the RBCs which is based on the combination of active rheology in optical tweezers and an analysis of forced RBC motion when the cell is optically trapped. This approach allows marking out correlated displacements of trapped erythrocyte edges. The displacements determined using forced vibrations analysis in the frequency range up to 1 kHz quantitatively characterize the viscoelastic properties of individual RBC. A new dynamic parameter, namely, the tangent of phase difference in the movement of the erythrocyte edges, is introduced as an effective finger-print characterizing the state of the cell.

Further author information: (Send correspondence to Andrey A. Fedyanin)

Andrey A. Fedyanin: E-mail: fedyanin@nanolab.phys.msu.ru, Telephone: +7 495 939 39 10

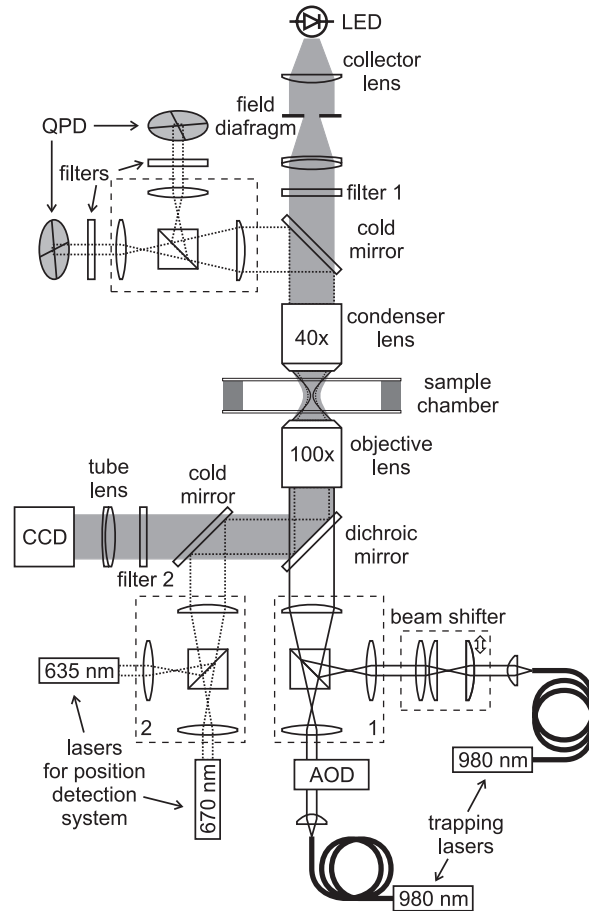


Figure 1. Sketch of the experimental setup: double-trap optical tweezers for RBC elastic properties monitoring. 1, 2 — systems for the conjugation and expansion of the laser beams.

2. MATERIALS AND METHODS

Figure 1 shows the setup of the double trap optical tweezers used in the experiments for RBC elastic properties monitoring. Two independent optical traps were formed using two singlemode diode infrared lasers (Lumics LU0975M330, Germany) with wavelength of 980 nm, output power of up to 330 mW. These laser diodes were pigtailed by polarization-maintaining optical fiber, and output radiation was collimated by aspheric lenses. After collimation one of laser beams was put through the beam shifter. The translation of the micrometer changed the position of the first shifter lens perpendicular to the optical axis which caused the movement of the trap within the focal plane of the focusing objective with translation accuracy about 30 nm per graduation of micrometer drive which results in precise control of optical trap position. The position of the second optical trap was controlled using acousto-optic deflector (Isomet LS55-NIR, USA). An oil immersion objective (Olympus UPLFLN 100XOI2, Japan) with numerical aperture of 1.3 and about 60% optical transmittance at 980 nm was used for focusing of the laser beams to form the traps. The objective working length was 0.15 mm when using 0.17 mm coverslip. This guaranteed the possibility to work with the sample throughout its thickness. Both laser beams were expanded to the full objective aperture to create maximal optical field gradient at the focal points for the most efficient RBC trapping. Laser beam expansion systems 1 and 2 are shown in Fig.1. They served as conjugating systems as well. The setup provides an accurate three-coordinate (relatively to the optical traps) sample positioning using step-motors. Two extra laser beams (635 nm and 670 nm) with the output power of 0.3 mW were used in order to detect small displacements of the trapped cell. The latter beams passed through the optical system controlling the positions and the width of the beams and then were focused into the sample. The

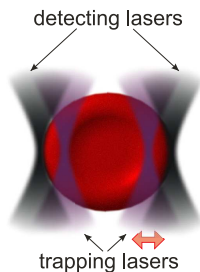


Figure 2. Single erythrocyte trapped by two infrared trapping lasers. One of the trapping lasers position is oscillating with an amplitude of 100 nm in the frequency range from 50 Hz to 1 kHz which is schematically shown by the arrow. Two extra lasers which are focused on the RBC edges are used for the RBC edges positions detection.

forward scattered light was collected by a 40x objective and detected using two quadrant photodiodes (QPD). Displacements of the trapped cell were extracted from the changes in the QPD photocurrent. White LED, collector lens and field diaphragm were used as the sample illuminating system. CCD camera was used for visual control of the trapped objects. Filter 1 absorbs the light with the wavelength more than 600 nm so that there were no artifactual spectral components detected by the QPDs. Filter 2 was used to prevent the infrared laser components from the traps to be detected by the CCD camera. The hermetic observation chamber was made of RBC suspension in autologous plasma placed between two coverslips. The coverslips were previously processed using the following protocol. They were firstly treated with a surface active agent, rinsed with deionized water with resistivity 18.2M Ω m. Then the coverslips were washed in ethanol with the volume fraction of 96%, in 3% hydrogen peroxide and after that were treated by bovine serum albumin with the concentration of 1 mg/ml. Fresh blood was taken from donors by a fingertip needle prick. For sample preparation 0.2 μ l of blood was suspended in 1 ml of autologous plasma, which was previously obtained by whole venous blood centrifugation (firstly 3500 RPM, 25°C, 7 min, then 20000 RPM, 25°C, 7 min). Centrifugation was carried out in order to purify plasma from formed elements of the blood including platelets that can be trapped together with RBCs preventing correct measurements. Then 40 μ l of the RBC suspension was placed into the hermetic observation chamber made of two 0.1 mm-thick coverslips separated by a gap of about 0.15 mm. The observation chamber was placed on the two-coordinate motorized stage for fine sample positioning in the focal plane. All measurements were performed at room temperature (25°C).

The use of the QPDs and extra-lasers is a handy tool for the trapped objects displacements monitoring. This method is particularly sensitive for measuring displacements of the trapped spheric objects at the nanometer scale. But the exact calculation of the displacements and optical forces acting on particles is difficult since the calculations can only be performed using approximate methods. They are only applicable within their ranges of validity. One of the main problem here is that the trapped object has to be spherical and isotropic. The scattering pattern from the nonspheric trapped object, for example from the cell, is complex that restricts the direct measurement of displacements in the trap. Another way to quantitatively analyze the movement of the trapped cell is to measure the relative to the trap oscillations phase of the cell's edge movement.

In the experiment single erythrocyte was doubly trapped at the edges by two independent laser tweezers with the cell being not stretched or deformed as it is schematically shown in Fig.2. The distance between the traps was fixed to 7.5 μ m while the erythrocytes studied were always selected to be of 8 μ m in size. Trapping laser power in the focal plane was 20 mW per each trap which was enough for effective cell trapping but at the same time no heating effect was observed on the time scales of the experiment duration. One of the traps was stable while the position of the second one was oscillated with an amplitude of 100 nm in the frequency range from 50 Hz to 1 kHz using acousto-optical deflector. This caused the cell vibration and the displacements of the cell edges. Position detecting lasers were also focused on the RBC edges as it is shown in Fig.2 and the scattered light was detected by QPDs.

The data acquisition time T was set for each frequency of the trap oscillation. The signal obtained by each

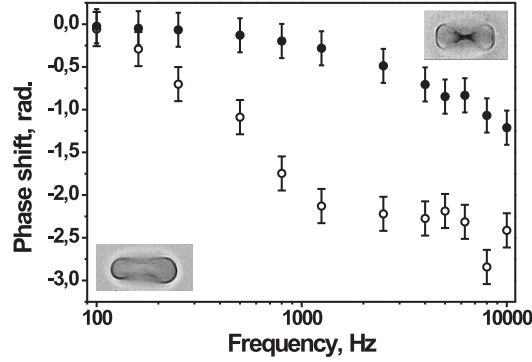


Figure 3. Dependence of the phase difference in the movement of the RBC edge in the fixed trap relative to the RBC edge trapped by an oscillating trap upon the frequency of the trap oscillation. Empty points correspond to the normal RBC, filled points relate to the cell fixed by glutaraldehyde (stiff membranes). Inset on the left shows a microphotograph of the trapped normal RBC. Inset on the right shows the microphotograph of the glutaraldehyde-fixed erythrocyte trapped in optical tweezers.

QPD is represented as follows:

$$f(t) = \frac{A_0}{2} + \sum_{k=1}^{\infty} (A_k \cos k\omega_0 t + B_k \sin k\omega_0 t) = \frac{A_0}{2} + \sum_{k=1}^{\infty} C_k \sin(k\omega_0 t - \varphi_k), \quad (1)$$

where

$$A_k = \frac{2}{T} \int_0^T f(t) \cos k\omega_0 t dt, B_k = \frac{2}{T} \int_0^T f(t) \sin k\omega_0 t dt, \quad (2)$$

$$C_k = \sqrt{A_k^2 + B_k^2}, \varphi_k = -\arctan \frac{A_k}{B_k}, \quad (3)$$

and $\omega_0 = 2\pi/T$. In the presence of external harmonical perturbation at the frequency $\omega = n\omega_0$ the phase φ_n characterizes the phase difference of the RBC edge displacement relative to the external perturbation. Provided by the cell edges displacements $f(t)_{1,2}$ the phase difference in the movement of the opposite edges of the RBC $\varphi = \varphi_{n2} - \varphi_{n1}$ referred to as phase difference (PD) further in the text can be obtained using Fourier transform, and the subscripts “1” and “2” refer to oscillating and fixed trap, respectively.

3. RESULTS AND DISCUSSIONS

The relative PD φ of the cell edges oscillations were measured as a function of the trap oscillation frequency ω . Figure 3 shows typical frequency dependences of the PD. Data-acquisition time for each data set was about 20 seconds for both directions of frequency increase and decrease. The results for different directions are almost identical, therefore the time impact during the measurements was neglected and the φ values for both directions were averaged. Experimental observations showed that dependence of the PD as a function of trap oscillation frequency considerably different for different types of the RBC membranes. Fig.3 shows that the PD of the glutaraldehyde-fixed erythrocytes shifts to the right comparing to the PD of the normal RBC. Glutaraldehyde solution (2.5%) is used as a fixative in biological applications.¹⁰ It makes the cells controllably rigid by crosslinking the proteins of the cell membrane.

In order to quantitatively characterize the elastic properties of the RBCs using this experimental approach the following phenomenological mechanical model shown schematically in Fig.4 was considered. It is determined by elastic elements k and K represented by springs, which describe the trap stiffness and the RBC elastic coefficient, respectively, and by purely viscous components γ and Γ represented by dash-pots describing the effective viscous

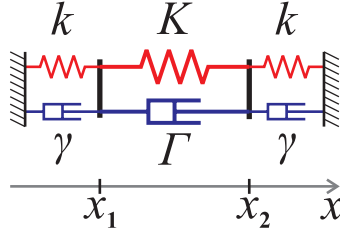


Figure 4. Phenomenological mechanical model of the trapped RBC, k is the trap stiffness, K is the RBC elastic coefficient, γ and Γ are effective viscous coefficients of the trapped system.

coefficients of a doubly trapped single erythrocyte. While the first trap oscillates forcing the trapped cell edge to move, the opposite cell edge faces the balance of the following viscous and elastic forces in its motion:

$$\gamma \dot{x}_2 = -k(x_2 - x_2^{\text{trap}}) + \Gamma(\dot{x}_1 - \dot{x}_2) - K(x_2 - x_1 - L), \quad (4)$$

where L is an undeformed K -spring length which is the RBC length, x_2^{trap} is a position of the second trap, x_1 and x_2 are the edges displacements from the trap centers.

The variables detected in the experiment are the displacements of cell edges from the equilibrium, $y_1 = x_1 - x_1^0$, $y_2 = x_2 - x_2^0$, where $x_{1,2}^0$ are the equilibrium positions of the opposite cell edges. The second cell edge movement is then described as follows:

$$(\gamma + \Gamma)\dot{y}_2 = \Gamma\dot{y}_1 - (k + K)y_2 + Ky_1. \quad (5)$$

Let the displacement of the cell edges from equilibrium to be of $y_1 = \hat{y}_1 \exp^{i\omega t}$, $y_2 = \hat{y}_2 \exp^{i\omega t}$. Solving Eq.(5) gives:

$$(k + K + i\omega(\gamma + \Gamma))\hat{y}_2 = (K + i\omega\Gamma)\hat{y}_1. \quad (6)$$

In assumption of the frequency range $\omega^2 \ll k(k + K)/\Gamma(\Gamma + \gamma)$ the PD tangent is written as follows:

$$\tan \varphi = -\frac{\Gamma k - \gamma K}{k(k + K)}\omega = -\omega\tau. \quad (7)$$

Phase difference tangent referred to as PDT further in the text appears to be a linear function of the trap oscillation frequency. The proportionality factor τ determines the viscoelastic properties of the trapped cell as a complex biological and hydrodynamical system where implementation of specific parameters is indispensable and it is impossible to pick out viscous and elastic cell properties independently. Having the dimension of time, the τ coefficient can be interpreted as an effective response time of the cell. It is related to the characteristic time of mechanical perturbation propagation in the cell. Experimental observations showed that dependence of the PDT as a function of trap oscillation frequency is reproducibly linear one and has considerably different slopes for different types of the RBC membranes which is shown in the Fig.5. Empty points in Fig.5 correspond to dynamic measurements for normal living RBC. The slope value appears to be of $(-6.4 \pm 0.1) \cdot 10^{-4}$ s. Filled points represent the measurements for the RBC previously fixed by glutaraldehyde. The slope value for glutaraldehyde-fixed RBC is equal to $(-2.7 \pm 0.2) \cdot 10^{-4}$ s. The error bar in the Fig.5 is a systematic experimental error which was approximately the same for all experimental points. Thermal undulations of the red cell membrane known as flicker phenomenon provide noise background to the frequency spectrum measured for a single RBC, which is optically trapped while one of the traps position is oscillating at the certain fixed frequency. Relative systematic error corresponded to the ratio of the amplitudes of adjacent noise Fourier harmonics to the amplitude of the peak at the frequency of applied perturbation. Therefore the response time τ measured for glutaraldehyde-fixed erythrocytes drastically decreases from $640 \mu\text{s}$ to $270 \mu\text{s}$ indicating considerable change in the state of the cell. This proves the ability of the offered method to detect and to control the effective rigidity of the cell.

It is important to mention that the equation (4) is written neglecting the mass of the object studied since the case of $m\omega^2 \ll k + K$ is considered. This estimation is supported by the following experiment.

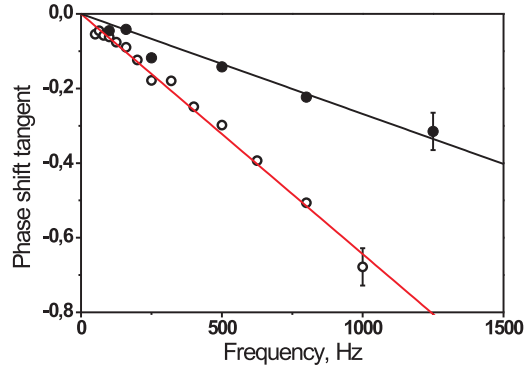


Figure 5. Dependence of the tangent of the phase difference in the movement of the RBC edge in the fixed trap relative to the RBC edge trapped by an oscillating trap upon the frequency of the trap oscillation. Empty points correspond to the normal RBC, filled points relate to the cell fixed by 2.5% glutaraldehyde (stiff membranes). Lines are linear mean-square fits to the data.

In order to estimate the trap stiffness k and effective elastic parameter K for the RBC, the trapping force calibration is needed first. For this carboxylated polystyrene beads, $3\ \mu\text{m}$ in diameter, were washed in phosphate buffer saline three times by centrifugation (Centrifuge 5417R, 3000 RPM, 25°C , 5 min). After that, RBCs and polystyrene beads were suspended in 1 ml of autologous plasma (~ 1 particle per RBC). The coverslips for observation chamber were treated by serum bovine albumin (BSA) solution to prevent RBCs from sticking to the glass. One bead and one RBC were trapped by two independent laser beams with a certain distance between them and were moved to the distance of $10\ \mu\text{m}$ above the lower coverslip. By varying the distance between the traps the particle and the cell were brought together until they contacted. The bead stuck irreversibly and nonspecifically to the RBC membrane in plasma within 1 to 2 min. Then the whole system was doubly trapped by the microbead and the opposite RBC edge. The trap power for the RBC edge was set at 20 mW and the trap power for the bead varied in order to find the laser power value which would equalize the trapping force of the microbead and the RBC edge. Escape trapping forces for the bead and for the RBC edge appeared to be the same when the trap power for the bead was of 17 ± 1 mW. In order to obtain the value of this force, standard escape force method was used. Aqueous glycerol solution (15% wt.) was chosen as a calibration medium. Its index of refraction appeared to be 1.351 with Abbe number $V = 42$, which was measured using the Abbe refractometer. The same index of refraction value was obtained for plasma. Since optical characteristics of glycerol solution mimic optical characteristics of plasma the trapping force of the calibration beads was expected to be the same in plasma and in glycerol. Provided by these characteristics, the same polystyrene particles as used in the previous measurements were suspended in glycerol solution and then trapped by optical tweezers at fixed height of $h = 10\ \mu\text{m}$ above the surface of the lower coverslip. As the optical trap moved, solution exerted a viscous drag force on the trapped bead which is given as $F = \beta \cdot v$, where β is a viscous drag coefficient for a spherical particle with the radius r in fluid at a height h from the surface:

$$\beta = \frac{6\pi\eta r}{1 - 9/16(r/h) + 1/8(r/h)^3 - 45/256(r/h)^4 - 1/16(r/h)^5}. \quad (8)$$

η was taken to be $1.32 \pm 0.02\ \text{mPa}\cdot\text{s}$ (room temperature 25°C). Viscous drag force was each time equal to the trapping force when the bead just escaped the trap. Provided by the value of the trap velocity v corresponding to this case, the trapping force of the bead in our glycerol solution was obtained and appeared to be $29 \pm 2\ \text{pN}$ for the laser power of 17 mW. Such approach to calibrate the optical trapping force was appropriate in our case as far as the Reynolds number was $\sim 10^{-3}$ (bead radius $r_{\text{bead}} = 1.50 \pm 0.05$, glycerol solution density $\rho = 1036\ \text{kg}/\text{m}^3$ – for 15% glycerol solution). As a consequence, escape trapping force of the RBC edge in plasma was estimated to be of $29 \pm 3\ \text{pN}$.

Provided by the RBC escape trapping force value the trap stiffness k for the RBC edge and effective RBC elastic parameter for small deformations K was estimated by doubly trapping a single erythrocyte and by

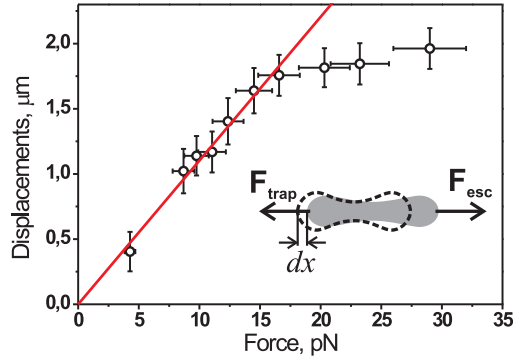


Figure 6. Dependence of the RBC edge displacement while pulling the traps apart upon the RBC edge trapping force F_{trap} . Solid line corresponds to the mean-square fit of the linear part of the data. The inset shows the schematic of the experiment, dx is the RBC edge displacement from its initial position in the fixed trap.

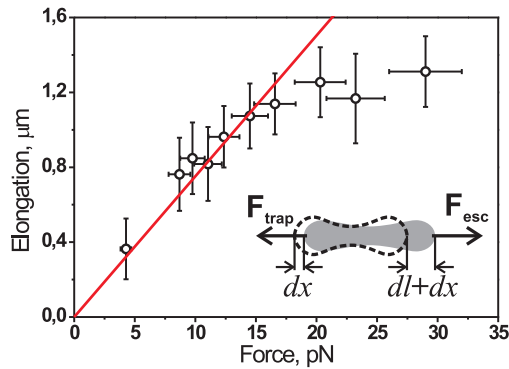


Figure 7. Dependence of the RBC elongation upon the trapping force while stretching the cell. Solid line corresponds to the mean-square fit of the linear part of the data. dl is the RBC elongation.

pulling one of the traps and keeping the other trap position fixed. This procedure was repeated for a numerous amount of erythrocytes and the resulted data obtained by means of optical microscopy were averaged over all the experiments. Fig.6 shows the dependence of the RBC edge displacement upon the RBC edge trapping force. For each data-point the maximal RBC edge displacement from its initial position in the fixed trap dx was detected before the cell slipped out from the trap. Approximation of the dependence linear part gives the value of the trap stiffness to be of about $9 \text{ pN}/\mu\text{m}$. At the same time the cell elongation dl was detected for each value of the trapping force shown in Fig.7. Linear fit gives the K value of about $13 \text{ pN}/\mu\text{m}$ which is of the same order as the k value. The maximal frequency value used in the experiment was 1 kHz . The blood test showed the value of the mean cell volume (MCV) to be of $88,5 \text{ fl}$, which is in correspondence with the normal MCV.¹⁹ Therefore the RBC mass is about 10^{-13} kg and the estimation of $m\omega^2 \ll k + K$ is reasonable for the case studied.

In optical tweezers experiments intense laser light is tightly focused therefore it is a matter of concern to be aware of photo-induced effects when biological samples are exposed to laser radiation. In our case a particular care was put to estimate photodamages induced by the traps and to provide the invasiveness of the method. For this, single erythrocyte was trapped by two opposite edges using optical tweezers. One of the traps was stable while the other one was oscillated at the frequency of 1 kHz with the amplitude of 100 nm . Displacements of the cell edges were detected as a function of experiment duration. The PD between oscillations of the opposite RBC edges was extracted. Time dependence of the PD with fixed frequency of forced oscillations shown in Fig.8 appears to be a constant at the scales of 160 seconds revealing no significant change in the cell form or viscoelastic properties during the experiment. This time is long enough since typical experiment duration is about 20 seconds.

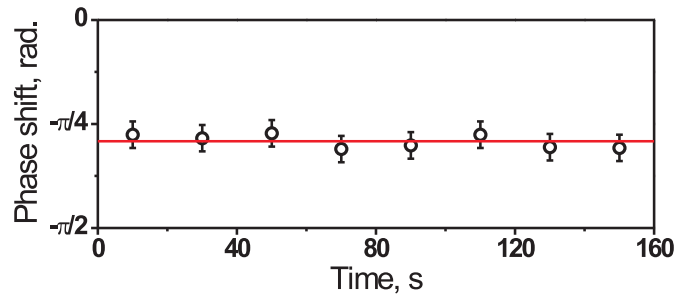


Figure 8. Time dependence of the phase difference between oscillations of the opposite RBC edges. Frequency of the trap oscillations is 1 kHz, amplitude of the trap oscillations is 100 nm.

4. CONCLUSIONS

Double trap optical tweezers are suggested as a method for precise monitoring of red blood cells viscoelastic properties using active rheology approach combined with the forced RBC edges vibration analysis. Tangent of the phase difference obtained while the cell is doubly trapped by the fixed optical trap and the trap oscillating at the specified frequency in the range from 50 Hz to 1 kHz appears to be an effective measure of the RBC viscoelastic properties. Phase difference tangent is found to be a reproducible linear function of the trap oscillation frequency that allows introducing a novel effective parameter – response time – characterizing the average viscoelastic properties of an individual cell. A significant difference in the response time is obtained for normal RBCs and the cells fixed by glutaraldehyde demonstrating the sensitivity of the offered method to the state of the cells. The photo-induced effects observed on typical experiment duration times are negligible.

ACKNOWLEDGMENTS

Authors gratefully acknowledge D. Petrov for invaluable advice, suggestions and helpful discussions on the initial stage of work. The research was carried out using CKP facilities, partially supported by M. V. Lomonosov Moscow State University Program of Development and financially supported by Russian Foundation of Basic Research and the Ministry of Education and Science of Russia.

REFERENCES

- [1] Neuman, K. and Block, S., “Optical trapping,” *Rev. Sci. Instrum.* **75**, 2787–2809 (2004).
- [2] Khokhlova, M., Lyubin, E., Zhdanov, A., Rykova, S., Sokolova, I., and Fedyanin, A., “Normal and SLE red blood cell interactions studied by double trap optical tweezers: direct measurements of aggregation forces,” *J. Biomed. Opt.* **17**, 025001 (2012).
- [3] Dao, M., Limb, C., and Suresh, S., “Mechanics of the human red blood cell deformed by optical tweezers,” *J. Mech. Phys. Solids* **51**, 2259–2280 (2003).
- [4] Fontes, A., Fernandes, H., Thomaz, A., Barbosa, L., Barjas-Castro, M., and Cesar, C., “Measuring electrical and mechanical properties of red blood cells with double optical tweezers,” *J. Biomed. Opt.* **13**, 014001 (2008).
- [5] Hochmuth, R., “Micropipette aspiration of living cells,” *J. Biomech.* **33**, 15–22 (2000).
- [6] Evans, E. and Yeung, A., “Apparent viscosity and cortical tension of blood granulocytes determined by micropipet aspiration,” *Biophys. J.* **56**, 151–160 (1989).
- [7] Evans, E., “Bending elastic modulus of red blood cell membrane derived from buckling instability in micropipet aspiration tests,” *Biophys. J.* **43**, 27–30 (1983).
- [8] Xu, W., Wood-Adams, P., and Robertson, C., “Measuring local viscoelastic properties of complex materials with tapping mode atomic force microscopy,” *Polymer* **47**, 4798–4810 (2006).
- [9] Mathur, A., Collinworth, A., Reichert, W., Kraus, W., and Truskey, G., “Endothelial, cardiac muscle and skeletal muscle exhibit different viscous and elastic properties as determined by atomic force microscopy,” *J. Biomech.* **34**, 1545–1553 (2001).

- [10] Marinkovic, M., Turner, K., Butler, J., Fredberg, J., and Suresh, S., "Viscoelasticity of the human red blood cell," *Am. J. Physiol. Cell Physiol.* **293**, C597–C605 (2007).
- [11] Dholakia, K. and Cizmar, T., "Shaping the future of manipulation," *Nature Photon.* **5**, 335–342 (2011).
- [12] Fazal, F. and Block, S., "Optical tweezers study life under tension," *Nature Photon.* **5**, 318–321 (2011).
- [13] Zhdanov, A., Kreuzer, M., Rao, S., Fedyanin, A., Ghenuche, P., Quidant, R., and Petrov, D., "Detection of plasmon-enhanced luminescence fields from an optically manipulated pair of partially metal covered dielectric spheres," *Opt. Lett.* **33**, 2749–2751 (2008).
- [14] Lyubin, E., Khokhlova, M., Skryabina, M., and Fedyanin, A., "Cellular viscoelasticity probed by active rheology in optical tweezers," *J. Biomed. Opt.* **17**, 101510 (2012).
- [15] Mizuno, D., Tardin, C., Schmidt, C., and Mackintosh, F., "Nonequilibrium mechanics of active cytoskeletal networks," *Science* **315**, 370–373 (2007).
- [16] Yoon, Y., Hong, H., Brown, A., Kim, D., Kang, D., Lew, V., and Cicutta, P., "Flickering analysis of erythrocyte mechanical properties: dependence on oxygenation level, cell shape, and hydration level," *Biophys. J.* **97**, 16061615 (2009).
- [17] Evans, J., Gratzer, W., Mohandas, N., Parker, K., and Sleep, J., "Fluctuations of the red blood cell membrane: relation to mechanical properties and lack of atp dependence," *Biophys. J.* **94**, 41344144 (2008).
- [18] Meiners, J. and Quake, S., "Direct measurement of hydrodynamic cross correlations between two particles in an external potential," *Phys. Rev. Lett.* **82**, 2211–2214 (1999).
- [19] Hashimoto, Y., Nakayama, T., Futamura, A., Omura, M., and Nakahara, K., "Erythrocyte mean cell volume and genetic polymorphism of aldehyde dehydrogenase 2 in alcohol drinkers," *Blood* **99**, 3487–3488 (2002).